THE INTERACTION OF ATOMIC OXYGEN WITH COPPER:

AN XPS, AES, XRD, OPTICAL TRANSMISSION AND STYLUS PROFILOMETRY STUDY

Ganesh N. Raikar, John C. Gregory and Ligia C. Christl
The University of Alabama in Huntsville
Huntsville, AL 35899.
Phone: 205/895-6076, Fax: 205/895-6819

Palmer N. Peters
ES64, Space Science Laboratory
NASA, Marshall Space Flight Center
Huntsville, AL 35812.
Phone: 205/544-7728, Fax: 205/544-7754

ABSTRACT

The University of Alabama in Huntsville (UAH) experiment A-0114 was designed to study the reaction of material surfaces with LEO atmospheric oxygen. The experiment contained 128 one inch circular samples; metals, polymers, carbons and semiconductors. Half of these samples were exposed on the front of the LDEF and remaining on the rear.

Among metal samples, copper has shown some interesting new results. There were two forms of copper samples : a thin film sputter-coated on fused silica and a solid piece of OFHC copper. They were characterized by x-ray and Auger electron spectroscopies, x-ray diffraction and high resolution profilometry. Cu 2p core level spectra were used to demonstrate the presence of Cu_2O and CuO and to determine the oxidation states.

Experiment No: A-0114

1: INTRODUCTION

We know that the environment at altitudes of 200-700 km, where satellites orbit the earth, is extremely harsh due to the presence of atomic oxygen. An understanding of the nature of hyperthermal atomic oxygen with materials is essential to the design of long-lived satellites. In this regard the Long Duration Exposure Facility (LDEF), which carried samples of metals, alloys, ceramics, polymers, semiconductors, paints and a host of other materials and remained in space for nearly six years, is proving to be a source of data unrivalled in the history of space flight [1].

The copper samples, in both thin film and solid forms, were flown on the leading edge, C9 tray of LDEF with matching trailing edge samples in the C3 tray. The trailing C3 samples showed little effect of atomic oxygen. In this paper we discuss the effect of atomic oxygen seen on the C9 samples.

The surfaces of most metals and alloys in contact with the atmosphere are covered by a thin layer of oxide which protects the underlying metal. A knowledge of the composition, structure and thickness of this oxide layer is vital in understanding the relationship between the surface and the properties of various metals such as adhesion, corrosion resistance and optical performance. Its use in space is of interest because of its similarity to silver, which has superior electrical properties but catastrophically poor resistance to atomic oxygen.

Copper has been one of the elements most extensively studied in the laboratory with several surface sensitive techniques. Interpretation of oxide spectral structures is easier for copper than for other transition metals. The x-ray photoelectron core level line-shapes of Cu in copper-oxide based compounds have been widely studied in recent years. After the discovery of copper oxide based high temperature superconductors, great interest has been prompted in the understanding of the electronic structure of the Cu-O bond [2].

Copper is known to form two common oxide phases, depending on the oxidation conditions: cuprous oxide (Cu_2O) and cupric oxide (CuO) whose properties are listed in Table 1. Cuprous oxide is a semiconductor with a band gap of 2.17 eV and has essentially a full 3d ($3d^{10}$) shell while cupric oxide is an antiferromagnetic semiconductor with a band gap of 1.4 eV and has an open 3d ($3d^9$) shell. Cuprous oxide is the most stable at low oxygen pressures, particularly under vacuum conditions, and is the main phase formed at room temperature in contact with the atmosphere. Cupric oxide grows only at higher temperatures in the presence of high enough pressures, and is found to reduce to Cu_2O when heated under vacuum [3]. An unstable cupric hydroxide $Cu(OH)_2$

also exists on some surfaces due to moisture absorption. An understanding of these three compounds which are the likely surface products of the corrosion of copper metal is thus important.

ESCA (Electron Spectroscopy for Chemical Analysis) has proved to be a very powerful tool in the identification of metallic Cu [Cu(0)], Cu_2O [Cu(I)], and CuO [Cu(II)] species through the analysis of the Cu (2p) peaks and of the corresponding "shake-up satellites", as well as the x-ray excited Auger Cu $L_{2,3}M_{4,5}M_{4,5}$ [4]. In this study, we have utilized x-ray photoelectron spectroscopy (XPS), x-ray excited Auger electron spectroscopy (AES), high resolution stylus profilometry, scanning optical microdensitometry, electrical measurements and x-ray diffraction techniques.

2: EXPERIMENTAL

Thin films of copper were prepared at Space Sciences Laboratory, NASA Marshall Space Flight Center. Substrates were fused silica optical flats, obtained from Acton Research Corporation. These were coated with ca. 68 ± 1 nm copper using an RF sputtering system. The solid copper sample was cut from OFHC copper rod of one inch diameter and polished with 1 μm diamond powder. XPS was used to monitor the surface cleanliness of all these samples.

X-ray diffraction measurements were made using a Rigaku x-ray diffractometer with a thin film attachment. The angle between the thin film sample and the x-ray beam was constant at 1 degree to maximize surface sensitivity.

We used a Taylor-Hobson Talystep, Model # 223-27 instrument for profilometer measurements only on the thin film sample. Both exposed and unexposed areas could easily be scratched down to substrate interface with a fine tungsten wire. The square negative pulse-like traces gave good indications of the thickness of the exposed and unexposed regions at several locations across the sample [5]. This technique could not be used on the solid metal sample.

Transmission measurements were made using a white light source and scanning microdensitometer to verify uniformity of the exposed and unexposed areas. Additional transmission measurements were made using 4 different colored filters in a densitometer with 1 mm diameter aperture, but with the sample slightly elevated above the aperture by a shim support at the edges to avoid physical contact with the copper film; calibration standards were similarly supported and included a bare substrate.

XPS and x-ray excited AES measurements were made with a Perkin-Elmer 5400 ESCA system with an Apollo 4500 Domain series workstation. Typical operating conditions were:

System Pressure:	2-5 x 10^{-9} Torr
Anode (Mg $K\alpha_{1,2}$,1253.6 eV)Power:	300 watts (15 kVand 20 mA)
Area of Analysis:	1.2 mm^2
Pass energy:	89.5 eV (XPS survey scans)
	17.9 eV (XPS multiplex, Auger lines)
	8.95 eV (XPS core lines)
Take-off angle:	45°

Sample charging was measured by the displacement of the adventitious surface C 1s peak at 284.8±0.2 eV. The reproducibility of the peak positions obtained was within ±0.2 eV. The effect of the Mg $K\alpha_{3,4}$ satellites has been removed from the Cu 2p peaks and the Auger line-shapes.

3: RESULTS AND DISCUSSION

3.1: X-Ray Diffraction

Figure 1 shows the x-ray diffraction pattern of the unexposed region of the copper thin film. Three main peaks at $2\theta = 36.5°$ (Cu_2O), 43.5° (Cu) and 50.5° (Cu) are observed. The intense main peak at 21° is due to the fused silica substrate. The data is interpreted as characteristic of metallic Cu with a thin film of Cu_2O on its surface.

Figure 2 shows the XRD pattern of the exposed region. There are three main peaks at $2\theta = 36.5°$ (Cu_2O), 43.5° (Cu) and 50.5° (Cu) with a small peak at 39° (CuO) plus the intense silica peak as seen before. The observed distribution of phases for this region can be described as a mixture of mainly Cu_2O and metallic Cu with some CuO being present.

3.2: Stylus Profilometry

It has been shown in a previous paper [5] that the stylus profilometer can be used to measure changes in the roughness, erosion depths and material growth on a flat surface. This technique has the unique ability to measure a range of dimensional changes from 1mm to 0.1 nm. If the molar

volume of metal oxide produced is different from that of the native metal, as is usually the case, the method is capable of detecting extremely low levels of oxidation.

Figure 3 shows a representative trace taken on the unexposed region showing a film thickness of ca. 68± 1 nm. Figure 4 shows that the thickness of the exposed region was 105.3 ±1 nm, or 40% greater than the unexposed region. The average height of the step measured at the mask edge as shown in Fig.5 was ca. 34.3±0.5 nm , in agreement with the difference in total film thickness.

If all the copper in the 68 nm film were converted to one or other of the oxides, the thickness of these oxide films would be 114 nm for Cu_2O and 117 nm for CuO. This calculation assumes the theoretical maximum densities for the solids (see table 1) . Since the exposed film is only 105 nm thick, we may assume that the metal is not entirely oxidized through to the substrate. Although the profilometry data cannot distinguish between the two oxides, the XRD analysis clearly shows a mixture of Cu_2O and native metal, but cannot be used quantitatively. Again assuming theoretical densities we calculate that the exposed film consists of 92 nm of Cu_2O and 13 nm of Cu. Thus 55 nm of Cu were oxidized during the full LDEF exposure.

3.3: Optical Measurements

Visual inspection of the copper film shows that the exposed portion is much more transmissive than the unexposed. White light optical density measurements on the unexposed and exposed portions of the copper film gave transmissions of 5 and 13% respectively. The transmittance and reflectance versus thickness of a pure copper film were calculated [6] using equations for normal incidence from air onto a homogeneous copper film on fused silica; corrections for contamination were neglected. Optical constants for pure copper and its oxides were used in separate calculations, assuming a single film on a fused silica substrate.

A pure copper film with the measured optical density of the exposed portion should be less than 35 nm thick, as determined from Fig.6 while stylus measurements of the exposed area indicated 105.3 nm thickness. The same analysis was performed assuming a 100% Cu_2O film in the exposed area. Figure 7 shows that pure Cu_2O would be much more transparent than that observed for the exposed portion. This also suggests only partial conversion of the exposed copper film to copper oxide, although visually the film does not appear metallic in nature. This also supports the conclusion reached from the XRD and profilometry results on the thin film sample. More detailed analysis of the transmission and reflectance of these films has been made using a multi-layer model. The results have provided quantitative support of the profilometer and XRD data, but will be reported later.

3.4: Electrical Measurements

Limited resistivity measurements of the exposed and unexposed halves of the copper thin film were made with two-terminal contacts and a digital ohmmeter. Because contact resistances were not eliminated, only rough comparisons can be made; although the resistivity of the exposed area was higher than the unexposed area, it appeared to be too good a conductor to be cuprous oxide. Again incomplete conversion of copper to an oxide is indicated.

3.5: XPS and AES Measurements

For this study, we have made use of both photoelectron and Auger line shifts and changes in the lineshapes to determine the presence of various oxides on the thin film and solid samples of copper. The spectra were analyzed in terms of relative peak area intensities, full width at half maximum (FWHM), chemical shifts in the Cu $2p_{3/2}$ and Cu $2p_{1/2}$, Cu $L_3M_{4,5}M_{4,5}$ Auger lines and satellite structure associated with the Cu $2p_{3/2}$ peak.

Figure 8 shows the survey scans measured on the exposed and unexposed regions of the solid Cu. The atomic concentrations measured on the thin film and solid samples are tabulated in Table 2. Contaminants observed are C and Si. Silicone contamination on LDEF samples has been reported by several groups. Carbon contamination was roughly 50-60 % on all the samples which we attribute to hydrocarbon contamination.

The O 1s line (ca. 530 eV) has been extensively used in the analysis of oxide surface species. The line has a relatively narrow width and a symmetric shape. However, the presence of more than one species complicates the analysis and accurate fitting of the complex band combinations. It has been observed that the O 1s electrons in metal oxide species with a formal charge assignment of O^{2-} have a lower binding energy than in "adsorbed" oxygen which may be present in the formal modes of O_2^-, O_2^{2-} or O^- .

Normally chemical shifts of several eV are observed between the O 1s lines from a bulk oxide (O^{2-}), hydroxide (OH^-) or molecular water (H_2O). As shown in Fig.9 the O 1s spectrum taken from the exposed region of the solid sample, three main bands can be fitted. The peak A at ca. 529.5 ± 0.2 eV (FWHM= 1.1) is attributed to the main oxide O^{2-} species on the surface. The peak B at ca. 530.8 ± 0.2 eV (FWHM=1.32) arises from OH^- species while the wide intense peak C at ca. 532.5 ± 0.2 eV (FHWM=1.77) may be due to silica [7].

One major difference between the XPS spectra of Cu(I) and Cu(II) is the presence of prominent satellite structures called "shake-up" satellites on the high binding energy side of the Cu 2p lines in Cu(II) oxide. More generally, these effects have been associated with paramagnetic species. Cu(II) has a paramagnetic $3d^9$ structure while Cu(I) has a filled 3d subshell. Similar shake-up satellites occur on the 2p lines of copper halides and also in paramagnetic nickel independent of valence or stereochemistry [8]. These shake-up satellites arise due to the interaction between the Cu $2p_{3/2}$ core hole and the valence electrons. It is now well accepted that the mainpeak corresponds to a final state of $2p^5 3d^{10} \underline{L}$ (where $\underline{L}$ means a ligand hole) and the satellite to a $2p^5 3d^9$ final state. The structure seen in the Cu $2p_{3/2}$ satellite is a result of multiplet splitting in the $2p^5 3d^9$ final state [9].

Such satellites are seen only on the exposed region of the solid sample and are absent in the thin film sample. In Fig.10 we have plotted Cu 2p peaks measured from both exposed and unexposed regions of the thin film along with that taken from a pure Cu control. The FWHM of Cu $2p_{3/2}$ increases from nearly 1 eV in the control sample to 1.8 eV in the unexposed and exposed regions. The shape of Cu 2p peaks in the exposed and unexposed regions is quite similar to that from pure Cu (I) oxide. The B.E shifts for these peaks are less than 0.2 eV when compared with those from metallic Cu. Thus the species on both sides of the sample are mostly Cu_2O.

Similar comparison is made for the Cu 2p peaks in Fig.11 measured from both exposed and unexposed regions of solid copper. The shape and the FWHM of Cu $2p_{3/2}$ peak in the unexposed region are the same as on the exposed and unexposed regions of the thin film sample. We can infer from this observation that the oxide present on the unexposed region is similar in composition to Cu_2O oxide. The shake-up satellites that appear in the Cu 2p peaks measured on the exposed region are characteristic of CuO oxide. This is reinforced by a larger FWHM of the main peak (3.7 eV) , and a chemical shift of ca. 1.3 eV with respect to the metallic Cu(0) and Cu(I) species. Similar satellites have been observed by de Rooij from copper strips flown on LDEF [10].

Angle-resolved XPS (ARXPS) measurements can provide a surface composition of thin films [11]. The information depth is limited to 3λ where λ is the inelastic mean free path for electrons in the materials and typically 5 to 30Å. We have performed ARXPS measurements on all the samples. It is interesting to notice that as we increase the angle of collection of photoelectrons and probe deeper into the sample, we observe changes in the corresponding Cu 2p spectra from the exposed side of the LDEF solid copper sample as shown in Fig.12. In particular the satellite peaks, prominent at the outer surface and attributed to CuO, are observed to decrease to almost zero at maximum probing depth. As the maximum depth probed in the ARXPS [12] is about 7 nm, we roughly

estimate the thickness of CuO on the exposed region of the solid copper sample as ca. 2-3 nm, and beneath this depth the oxide resembles Cu_2O.

A detailed analysis of the Auger-line shape for those transitions involving valence electrons, in principle, should provide valance-band information and also effective Coulomb repulsion between the final two electrons in the Auger process . Now the Coulomb interaction for the Cu $L_3M_{4,5}M_{4,5}$ Auger line can be determined from the relation:

$$U_{eff} = E_{kin} - E_b(2p) - 2E_b(3d)$$

where $E_b(2p)$ is the Cu 2p binding energy and $E_b(3d)$ is the binding energy of the 3d electrons, and U_{eff} is the effective Coulomb interaction. Generally, if U_{eff} is less than twice the one-electron band width [Γ] as measured from XPS, the resulting LVV Auger spectrum is characterized as "band-like" and should have the same shape as a self-convolution of the density of electronic states within the valence band. If $U_{eff} \geq 2\Gamma$, electron correlation effects will be important and the resulting Auger transitions are termed "quasi-atomic", as they exhibit fine structure [13] as seen in the Cu Auger lines.

In Fig.13 we have plotted on a binding energy scale the Cu $L_{2,3}M_{4,5}M_{4,5}$ Auger spectra measured from the exposed regions of thin film and copper solid samples which are in turn compared with that from the Cu control. The scales are normalized to the C 1s fiducial at 284.6 eV. There are clear differences in these spectra. The Auger spectra from the LDEF samples are broader and lack the fine structure seen in the control sample. The two features marked A and B in the spectrum 3 (lab control) are "double ionization satellites" arising from the $L_2L_3M_{4,5}$ Coster-Kronig type of Auger transitions which results in a $3d^7$ final state. After this process has taken place, the created L_3 hole decays via the normal $L_3M_{4,5}M_{4,5}$ Auger process. The Auger spectral shape of spectrum 1 is different from that of spectrum 2. Also the intensity of the ionization satellites is considerably less in spectrum 1. It has been suggested that the shake-up $3d^9$ states which are responsible for the XP shake-up satellites in Cu (II) materials will enhance the intensity of the ionization satellites as seen in spectrum 2 [14]. The spectrum 2 thus identifies the presence of Cu (II) species in larger amount than in spectrum 1. The most prominent line in the Cu Auger $L_3M_{4,5}M_{4,5}$ spectrum and its energy is used for the chemical state identification. A peak shift of ca. 2.3 eV to lower kinetic energy (i.e higher binding energy) is observed between the Cu (0) and Cu (I) Auger lines, and nearly 1 eV between the Cu (0) and Cu (II) Auger lines as seen in the Fig.13. Again, we deduce that the surface copper species on the exposed portions of the solid sample and the thin film are Cu (II) and Cu (I) respectively.

4: SUMMARY

A battery of surface and thin film techniques has been applied to the analysis of the oxidized copper surfaces exposed in LDEF experiment A0114. These surfaces on row 9 received a total fluence of 8.72 $x10^{21}$ oxygen atoms per square cm.

XRD and high resolution profilometry have shown that on the thin film sample, 55 nm of copper was converted stoichiometrically to Cu_2O. Optical transmission measurements were consistent with this result. ESCA analysis has shown that the outermost layers of the cuprous oxide (ca. 2-3 nm) have been oxidized to a cupric oxide on the solid sample. This may be hydrated and in the form of $Cu(OH)_2$. It is our hypothesis that this oxidation from Cu (I) to Cu (II) occurred after the samples were returned to earth. The difference in re-oxidation between the two samples is probably due to different storage and analysis histories. The re-oxidation hypothesis has recently been substantiated by oxygen-18 isotope measurements by Saxon et al [15] on copper grounding strips. We note that our results and conclusions are entirely consistent with those of de Rooij [10], also made on the copper grounding strips.

5: REFERENCES

[1] Bland A. Stein and H. Gary Pippin, Proceedings of "First LDEF Post-Retrieval Symposium", Kissimmee, June 2-8, 1991; Ed. Arlene S. Levine, NASA CP-3134, P.617.

[2] P.A.P. Lindberg, Z.X.Shen, I. Lindau and W.E.Spicer, Surf.Sci.Rep., 11 (1991) 1.

[3] A.F. Wells, *Structural Inorganic Chemistry*, 5th Ed (Clarendon Press, Oxford, 1984) 1 ; A. Billi, E. Marinelli, L. Pedocchi and G. Rovida, Proceedings of 11th Int. Corrosion Congress, Florence, 1990, P.129.

[4] N.S. McIntyre, S. Sunder, D.W. Shoesmith and F.W. Stanchell, J. Vac. Sci. Technol. 18, (1981) 714; C. Malitesta, T. Rotunno, L. Sabbatini, and P.G. Zambonin, J. Chem. Soc. Faraday Trans. 86 (1990) 3607.

[5] Ligia C. Christl, John C. Gregory and Palmer N. Peters, Proceedings of "First LDEF Post-Retrieval Symposium", Kissimmee, June 2-8, 1991; Ed. Arlene S. Levine, NASA CP-3134, P.723.

[6] Hass, Georg, and Lawrence Hadley, "Optical Properties of Metals", in American Institute of Physics Handbook, Ed. D.E Gray et al (McGraw-Hill, N.Y, 1963), P.6.

[7] Terry L.Barr, J.Vac.Sci. Technol. A 9(3) (1991) 1793.

[8] G. van der Laan, C. Westra, C. Haas and G.A. Sawatzky, Phys. Rev. B 23, (1981) 4369.

[9] J. Ghijsen, L. H. Tjeng, J. van Elp, H. Eskes, J. Westerink, G. A. Sawatzky and M. T. Czyzyk, Phys. Rev. B 38 (1988) 11322.

[10] A. De Rooj, Proceedings of "Materials in a Space Environment", Cannes, Sept , 1991, P.119.

[11] C. S. Fadley, Prog. Solid State Chem. 2 (176) 265.

[12] I. Dalins and M. Karimi, J. Vac. Sci. Technol, A 10(4) 1992, 1.

[13] J. C. Fuggle in, "Electron Spectroscopy: Theory, Techniques and Applications", Vol.4, Eds. C. R. Brundle and A. D. Baker (Academic Press, N.Y, 1981) P.86.

[14] D.E. Ramaker, J.Electron Spectroscopy and Related Phen. 52 (1990) 341.

[15] J. M. Saxton, I. C. Lyon, E. Chatzitheodoredis, J. D. Gilmour and G. Turner, Presented at the "Second LDEF Post-Retrieval Symposium", San Diego, June 1-5, 1992; NASA CP-10067, P.78.

TABLE 1

Properties of Cu and Its Oxides

Species	Oxidation State	Color	Structure	Formula Weight	Specific Gravity	Refractive Index
Cu	0	Red	Cubic	63.5	8.92	-----
Cu_2O	+1	Red	Cubic	143	6.0	2.70
CuO	+ 2	Black	Monoclinic	79.5	6.3-6.5	2.63

TABLE 2

Surface Atomic Concentration

		Copper Thin Film, C9-16		Solid Copper, C9-30	
Photo Peak		Exposed	Unexposed	Exposed	Unexposed
Cu 2p	A.C (%)	4.3	2.7	8.9	5.6
O 1s	"	37.4	21.6	55.0	25.2
C 1s	"	44.4	65.8	18.5	62.9
Si 2p	"	13.9	9.3	16.9	4.9
Na 1s	"	0.0	0.0	0.0	0.5
Cl 2p	"	0.0	0.6	0.7	1.0

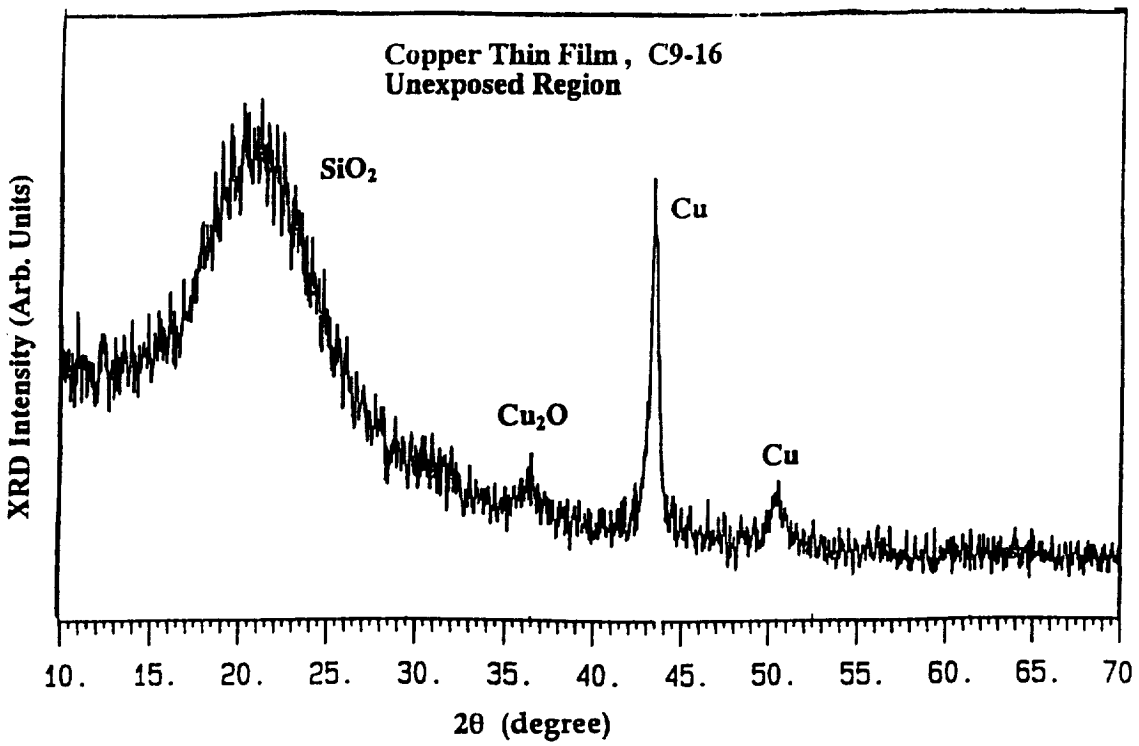

Fig. 1: XRD pattern of the unexposed region of Cu thin film.

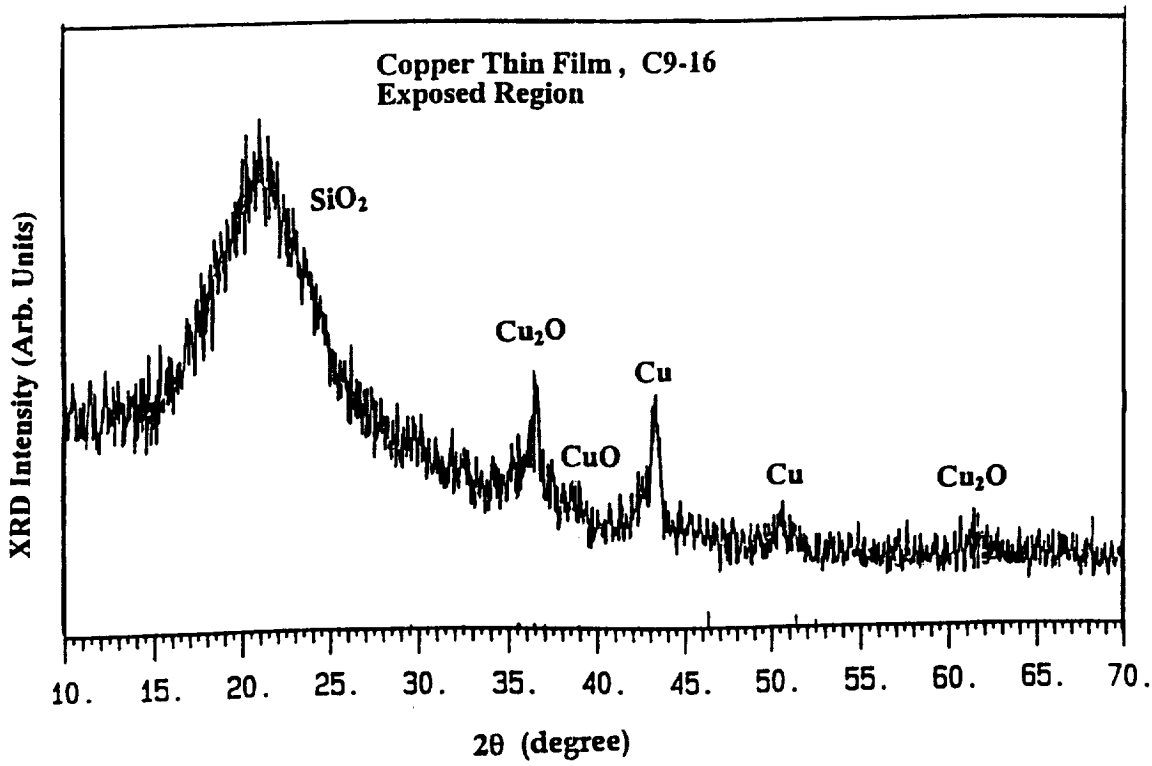

Fig. 2: XRD pattern of the exposed region of Cu thin film.

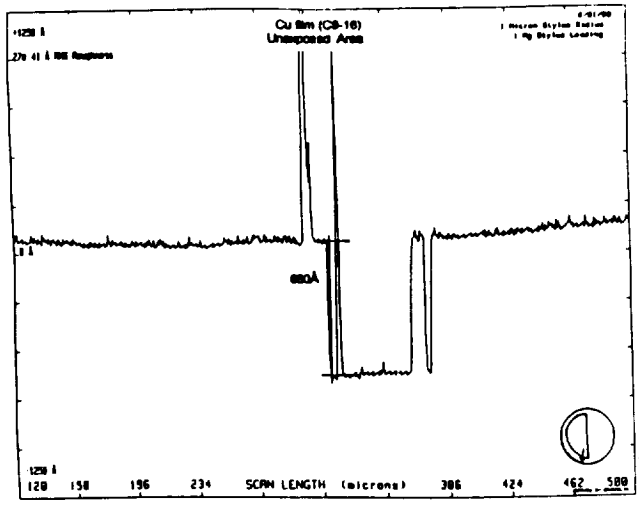

Fig. 3: Surface profile of the unexposed region of Cu thin film

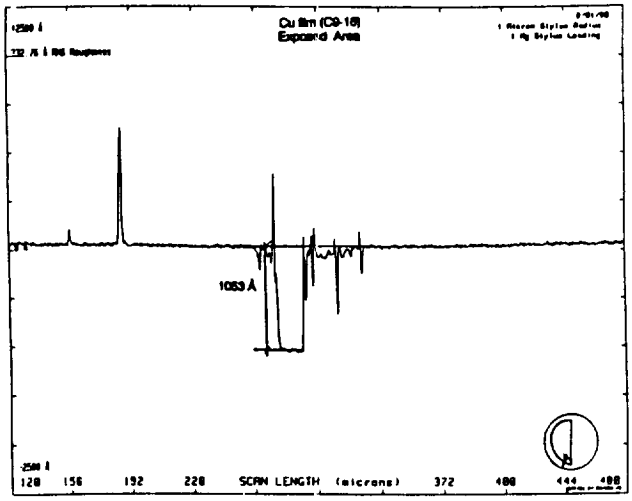

Fig. 4: Surface profile of the unexposed region of Cu thin film

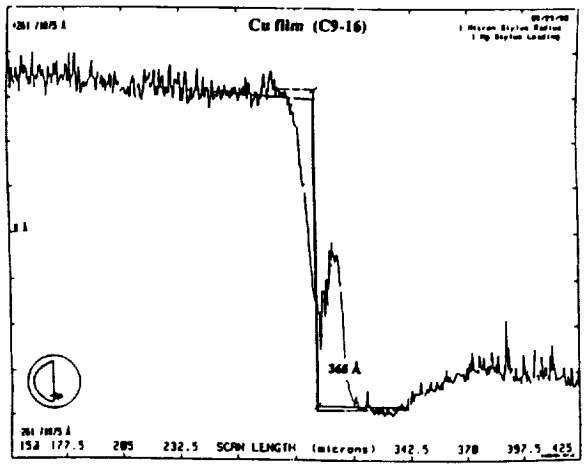

Fig. 5: Surface profile of transition from the exposed to the unexposed region of Cu thin film

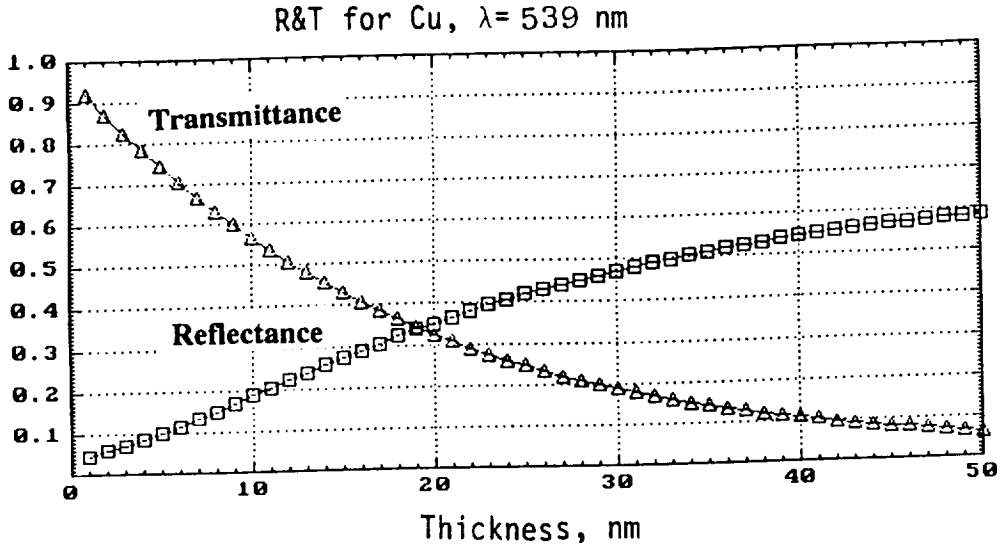

Fig. 6: Calculated Reflectance and Transmittance curves for Cu

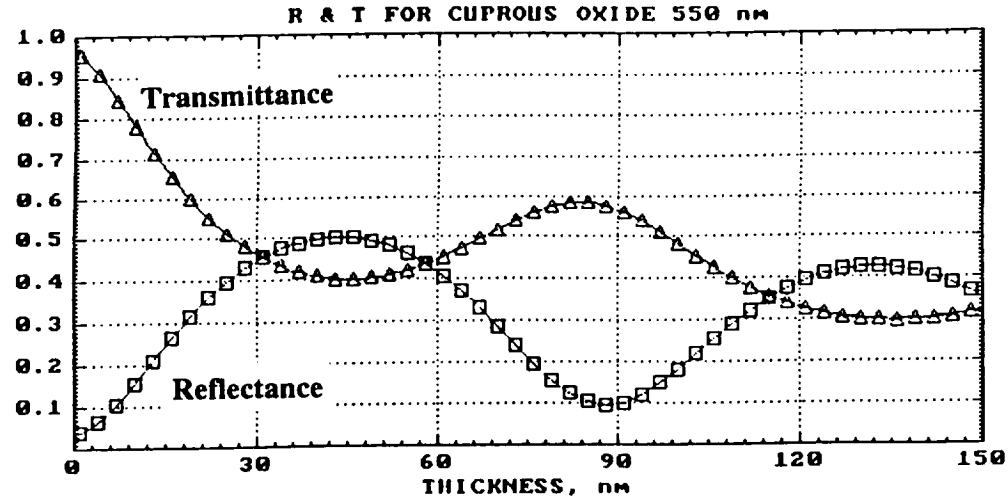

Fig. 7: Calculated Reflectance and Transmittance curves for Cu_2O

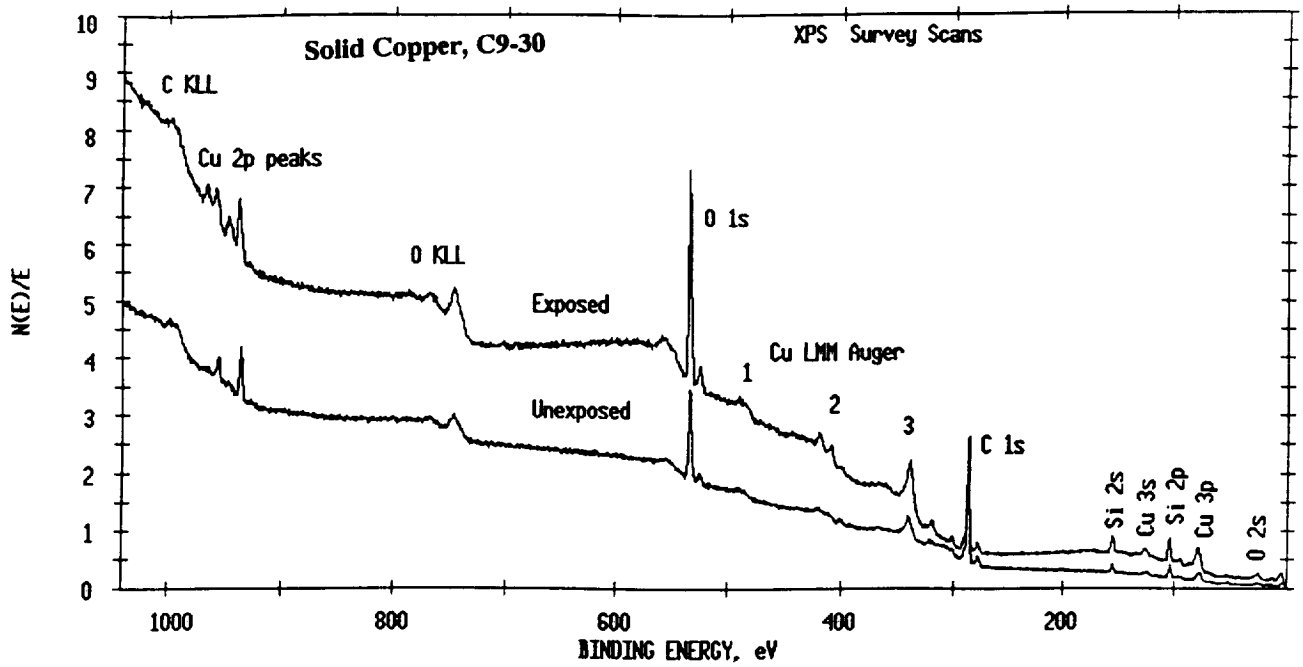

Fig. 8: XPS survey scans of the unexposed and exposed regions of Solid Cu

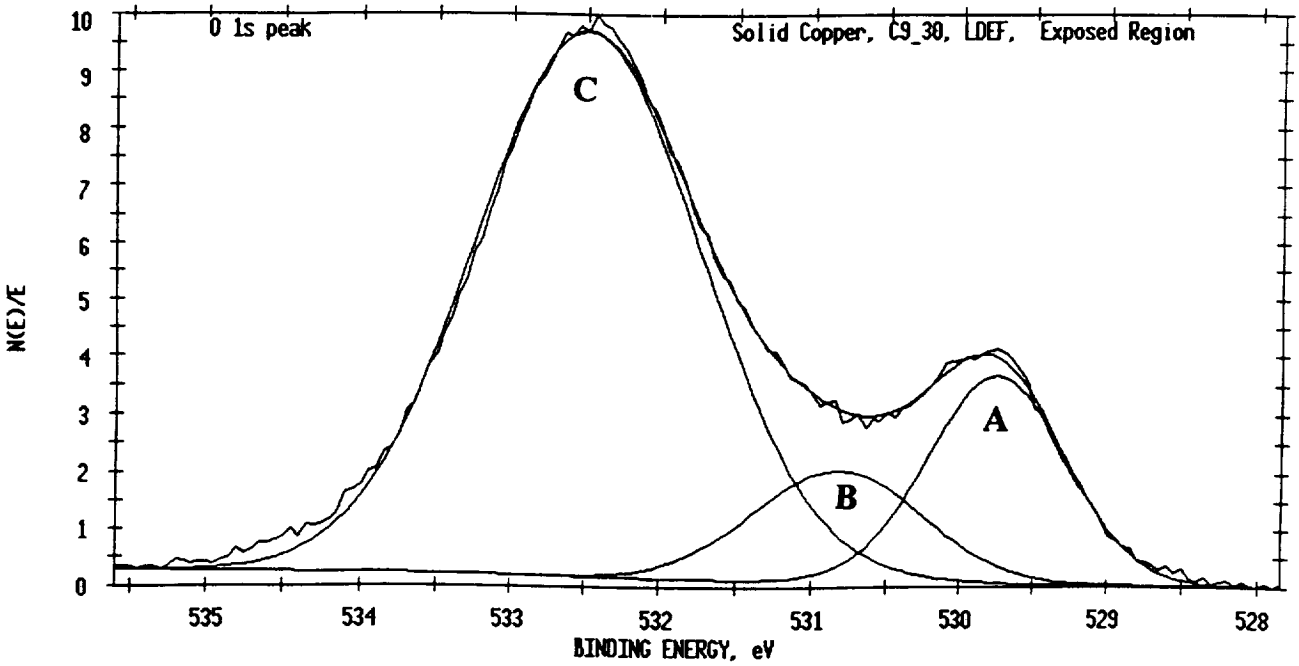

Fig. 9: Curve synthesis for the O 1s core-line from the exposed region of solid Cu

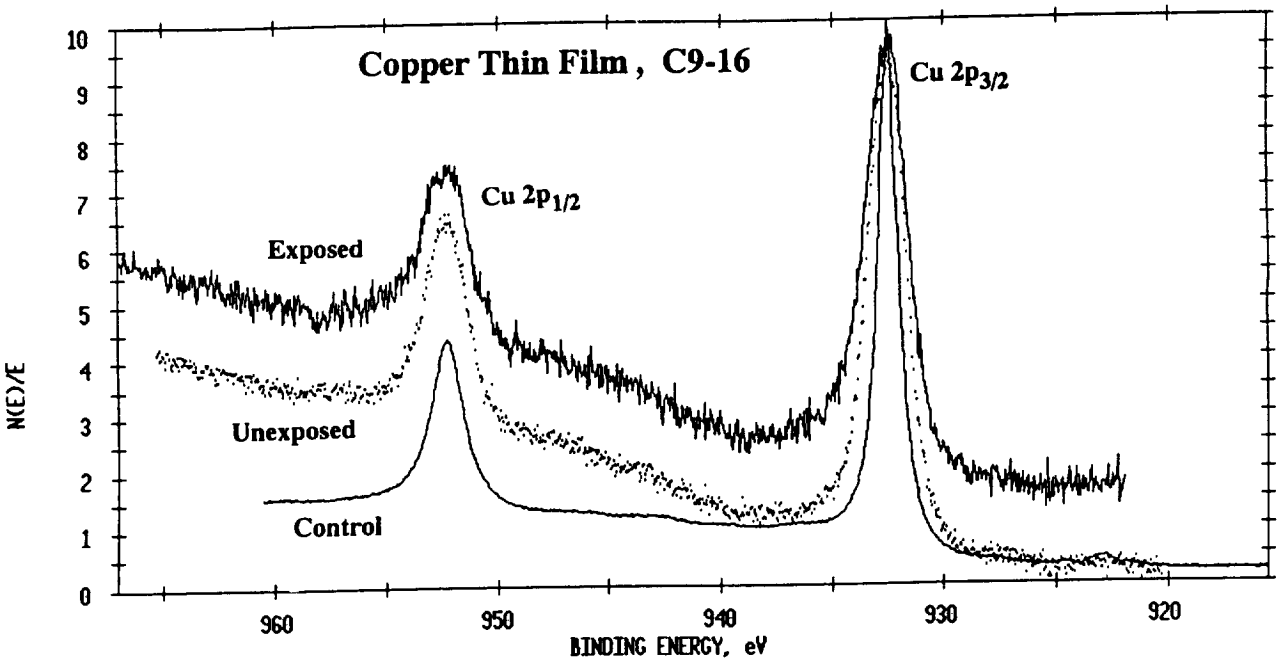

Fig.10: Cu 2p core-level peaks of the exposed and unexposed regions of Cu thin film

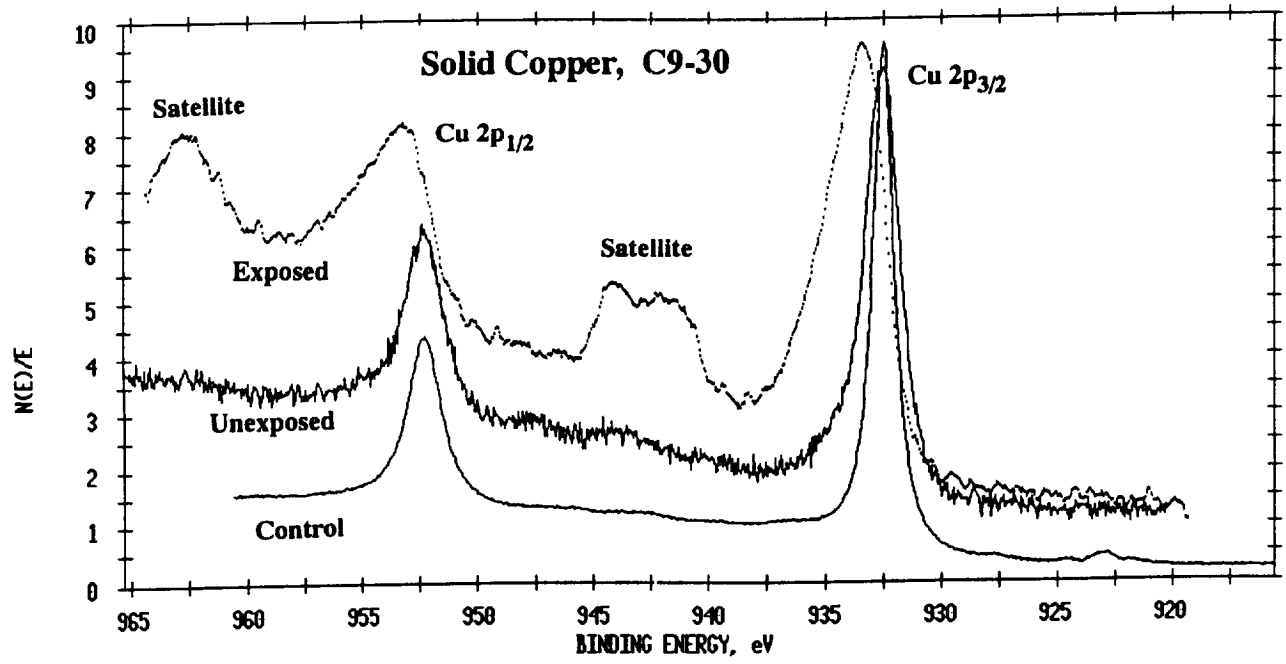

Fig. 11: Cu 2p core-level peaks of the exposed and unexposed regions of solid Cu

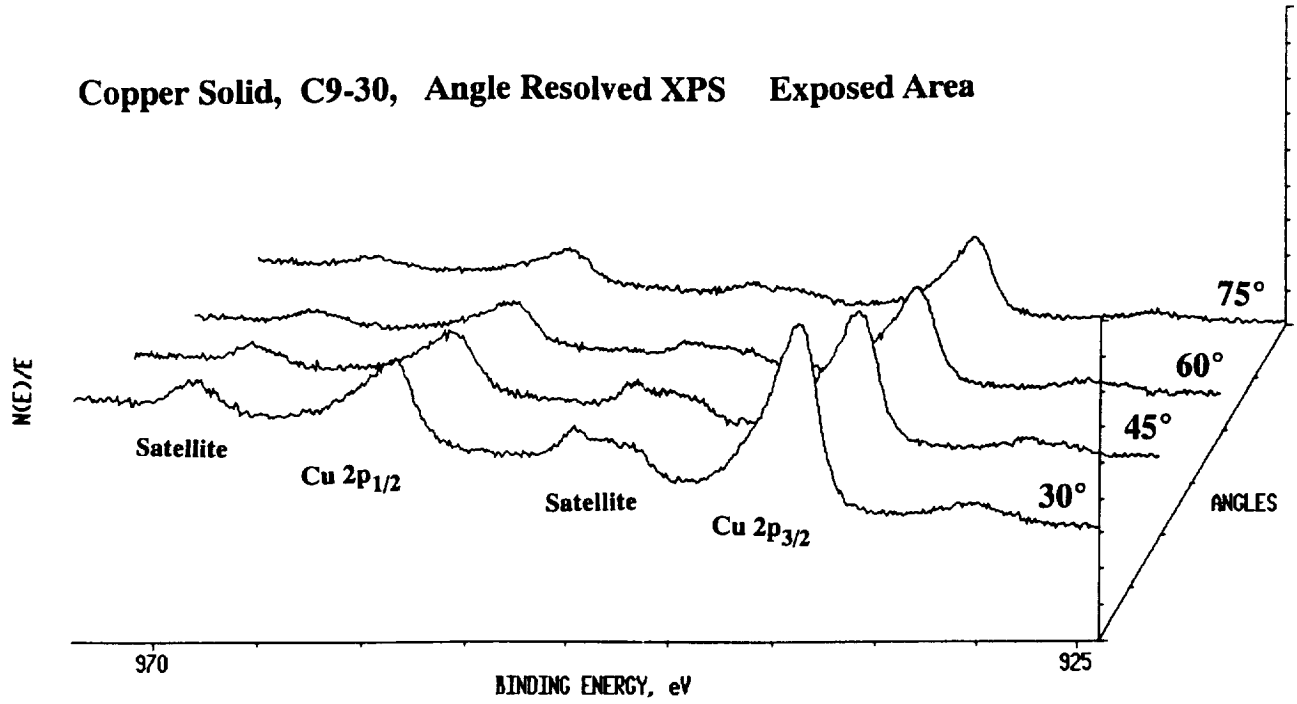

Fig. 12: Angle resolved XPS montage plot of Cu 2p core-level peaks of the exposed region of solid Cu sample. A larger take-off angle for the electrons correlates with a sampling depth deeper into the surface

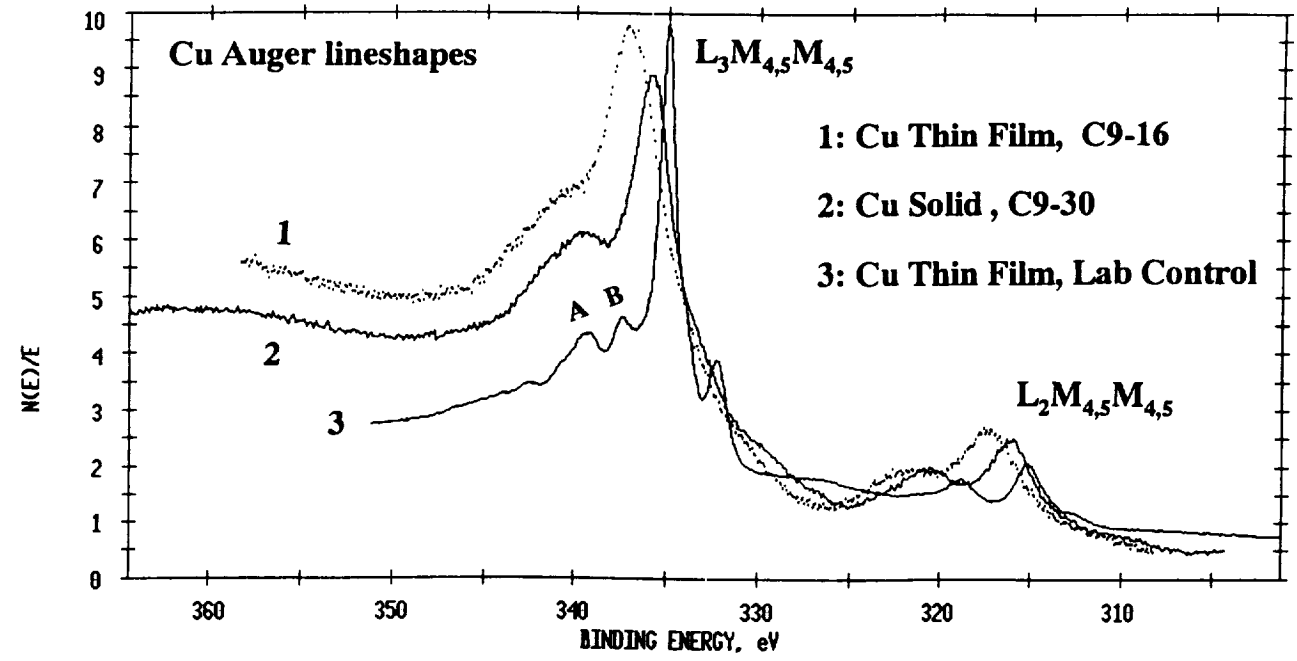

Fig. 13: Cu Auger ($L_{2,3}M_{4,5}M_{4,5}$) line-shapes of Cu thin film and solid Cu samples